


## RESEARCH ARTICLE

# A bioartificial kidney device with polarized secretion of immune modulators

N. V. Chevtchik<sup>1</sup> | M. Mihajlovic<sup>2</sup> | M. Fedecostante<sup>2</sup> | L. Bolhuis-Versteeg<sup>1</sup> |  
J. Sastre Toraño<sup>3</sup> | R. Masereeuw<sup>2</sup> | D. Stamatialis<sup>1</sup> 

<sup>1</sup>Bioartificial Organs, Department of Biomaterials Science and Technology, MIRA Institute for Biomedical Technology and Technical Medicine, University of Twente, Enschede, the Netherlands

<sup>2</sup>Division of Pharmacology, Utrecht Institute for Pharmaceutical Sciences, Utrecht University, Utrecht, the Netherlands

<sup>3</sup>Division of Chemical Biology and Drug Discovery, Utrecht Institute for Pharmaceutical Sciences, Utrecht University, Utrecht, the Netherlands

## Correspondence

Dimitrios Stamatialis, Bioartificial organs, Department of Biomaterials Science and Technology, MIRA Institute for Biomedical Technology and Technical Medicine, University of Twente, Enschede, the Netherlands.

Email: d.stamatialis@utwente.nl

## Funding information

EU-FP7-PEOPLE-ITN-2012 Project BIOART, Grant/Award Number: 316690; EuTox Working Group

## Abstract

The accumulation of protein-bound toxins in dialyzed patients is strongly associated with their high morbidity and mortality. The bioartificial kidney device (BAK), containing proximal tubule epithelial cells (PTECs) seeded on functionalized synthetic hollow fibre membranes, may be a powerful solution for the active removal of those metabolites. In an earlier study, we developed an upscaled BAK containing conditionally immortalized human PTEC with functional organic cationic transporter 2. Here, we first extended this development to a BAK device having cells with the organic anionic transporter 1, capable of removing anionic uraemic wastes. We confirmed the quality of the conditionally immortalized human PTEC monolayer by confocal microscopy and paracellular inulin-fluorescein isothiocyanate leakage, as well as by the active transport of anionic toxin, indoxyl sulphate. Furthermore, we assessed the immune safety of our system by measuring the production of relevant cytokines by the cells after lipopolysaccharide stimulation. Upon lipopolysaccharide treatment, we observed a polarized secretion of proinflammatory cytokines by the cells: 10-fold higher in the extraluminal space, corresponding to the urine compartment, as compared with the intraluminal space, corresponding to the blood compartment. To the best of our knowledge, our work is the first to show this favourable cell polarization in a BAK upscaled device.

## KEYWORDS

bioartificial kidney, cPTEC monolayer, living membrane, organic anionic transporter, polarized secretion of immune modulators

## 1 | INTRODUCTION

Despite the ongoing progress in dialysis therapy, only small- and middle-size xenobiotics can be eliminated. The removal of bigger size solutes and protein-bound toxins is limited (Krieter et al., 2009; Meyer et al., 2005). Recently, the accumulation of these protein-bound solutes has been strongly associated with the fatal outcome of the patients (Meijers et al., 2010; R. Vanholder, Schepers, Pletinck, Nagler, & Glorieux, 2014). Therefore, there is a strong need for novel strategies and concepts for their removal (Vanholder, Eloot, &

Glorieux, 2015), such as a bioartificial kidney (BAK). The BAK aims at mimicking the functional kidney by making use of proximal tubule epithelial cells (PTECs), equipped with a broad range of transporters, which normally mediate the excretion of those solutes (Masereeuw et al., 2014). This device consists of living membranes composing of tight monolayer of renal cells with preserved functional organic ion transporters, grown on an artificial porous hollow fibre membrane (HFM).

In recent years, several studies have presented BAK prototypes making use of human PTEC (Humes et al., 2002; Oo, Deng, Ni, &

Kandasamy, 2011; Oo, Kandasamy, Tasnim, & Zink, 2013; Saito et al., 2012; Sanechika et al., 2011; Sun et al., 2011; Takahashi et al., 2013; Tumlin et al., 2008), showing a preserved phenotype and sometimes metabolic and/or endocrine functions in vitro or in vivo. However, mostly primary cell lines were used, which are characterized by limited availability, donor-to-donor variation, and the loss of phenotype or functionality upon culturing. The recently developed and well-characterized human conditionally immortalized PTEC (ciPTEC) line appears to be a suitable candidate for an efficient BAK system (Chevtchik et al., 2016; Jansen et al., 2014; Jansen et al., 2015; Jansen et al., 2016; Nieskens et al., 2016; Schophuizen et al., 2015; Wilmer et al., 2010). These cells are transduced with human telomerase (hTERT) that limits replicative senescence by telomere length maintenance. In addition, their proliferation is controlled by the temperature sensitive mutant of SV40 Large T antigen (SV40tsA58), allowing proliferation at 33 °C and differentiation in mature PTEC at 37 °C. Due to these modifications, the cell line has high availability, limited senescence, and can be used up to a high passage number.

A recent study on small single HFM showed an active excretion of indoxyl sulphate (IS) and kynurenic acid by ciPTEC (Jansen et al., 2016) through the concerted action of organic anion transporter 1 (OAT1), breast cancer resistance protein, and multidrug resistance protein 4 (MRP4). This property of the ciPTEC is of high importance for BAK application, considering that most of the protein-bound toxins are anionic molecules (Miyamoto et al., 2011; R. Vanholder, De Smet, Glorieux, Argiles, et al., 2003). In the present work, we first developed an upscaled living membrane to support the OAT1-expressing ciPTEC line. The transport properties and the quality and function of the grown ciPTEC monolayer were investigated, including the expression of zonula occludens-1 (ZO-1) protein and the diffusion of fluorescein isothiocyanate (FITC)-labelled inulin (inulin-FITC). Furthermore, we studied the transport of an anionic uraemic toxin, IS, mediated by the combined action of OAT1, BRCP, and MRP4, in the absence or in the presence of the OAT1 inhibitor, probenecid.

A very important issue related to the clinical implementation of the BAK device is its safety. It is crucial to investigate whether the device with the human allogenic cells induces immune and inflammatory responses in the host. Besides, the high uraemic toxins concentrations in kidney patients are often associated with inflammation, which may as well be detrimental for the BAK (Hsu et al., 2014). A first assessment of the immunogenicity of the ciPTEC lines using flat membranes with a small surface area (1.12 cm<sup>2</sup>) showed that ciPTECs have low immunogenicity in vitro, although able to secrete several proinflammatory cytokines that could potentially mediate a non-specific inflammatory response (Mihajlovic et al., 2017). In this work, we investigated whether there is polarization of the production of proinflammatory and immune mediators by the ciPTEC cultured in the BAK system. We measured the release of the most relevant proinflammatory mediators—IL-6, IL-8, and TNF- $\alpha$ —and soluble HLA (sHLA)-Class I without or with exposure to lipopolysaccharide (LPS) or interferon- $\gamma$  (IFN- $\gamma$ ) in both—dialysate and blood—compartments of the system. To the best of our knowledge, our work is the first to focus on this important issue for the development of BAK devices.

## 2 | MATERIALS AND METHODS

### 2.1 | Chemicals

All chemicals were purchased from Sigma-Aldrich (Zwijndrecht, The Netherlands) unless stated otherwise. MicroPES TF10 hollow fibre capillary membranes (HFM; wall thickness 100  $\mu$ m, inner diameter 300  $\mu$ m, max pore size 0.5  $\mu$ m) were purchased from 3 M—Membrana GmbH (Wuppertal, Germany).

### 2.2 | Module preparation, HFM sterilization, coating, and characterization

The modules were prepared following the protocol presented previously (Chevtchik et al., 2016). A dual coating of L-Dopa and Collagen IV coating was applied to the fibres, at 37 °C on a shaking device, for a duration of 20 and 2 h, respectively (Chevtchik et al., 2016). The HFM transport properties (water permeability) was measured before and after sterilization and before and after coatings, in the absence of ciPTEC. In fact, we used an OSMO Inspector automated set-up (Convergence B. V, Enschede, The Netherlands) to quantify the clean water (Merck Millipore, Billerica, MA) flux (CWF) through the HFM ( $J$ , in L/(m<sup>2</sup>·h<sup>1</sup>)) as a function of the transmembrane pressure (TMP or  $\Delta P$ , in bar). The membrane permeance ( $L$ , in L/(m<sup>2</sup>·h<sup>1</sup>·bar<sup>1</sup>)) was calculated from the slope of this curve. Every pressure step was maintained for 30 min.

#### 2.2.1 | Cell culture and modules handling

The ciPTEC OAT-1 expressing, urine-derived, cell line (Nieskens et al., 2016; Wilmer et al., 2010) was cultured at 33 °C proliferating temperature and at 37 °C maturation temperature in ciPTEC complete medium. The latter was prepared as described previously (Chevtchik et al., 2016) with the difference that ciPTECs were always cultured in the absence of antibiotics up to a maximum of 60 passages. The modules' handling and cell seeding were performed as reported previously (Chevtchik et al., 2016). Briefly, prior to cell seeding, modules were incubated for 1 hr in ciPTEC complete medium. Proliferating 90% confluent ciPTECs were detached using Accutase (StemPro® Accutase®, Life Technologies Europe BV, Bleiswijk, The Netherlands), centrifuged and suspended at a concentration of 2.0–2.5 million cells/ml in the ciPTEC complete medium. The modules' extraluminal space was completely filled with the cell suspension. To promote initial cell attachment, the modules were placed at 33°C, 5% CO<sub>2</sub> for 8 hr, with a rotation of 90° every 2 hr. Afterwards, the modules were washed with the ciPTEC complete medium, provided with gas exchange filters, and the cell proliferation was allowed for additional 64 hr. Finally, the temperature was changed to 37 °C for 7 days to allow ciPTEC maturation. During the culture period, ciPTECs were supplemented with fresh culture medium every second day.

#### 2.3 | Immunochemistry

Matured ciPTECs were fixed using 2 w/v% paraformaldehyde in Hanks Balanced Salt Solution (HBSS) supplemented with 2 w/v%

sucrose for 10 min and permeabilized in 0.3 v/v% triton X-100 in HBSS for 10 min. To prevent non-specific binding of antibodies, cells were exposed to block solution containing 2 w/v% bovine serum albumin, 2 v/v% fetal calf serum, and 0.1 v/v% tween-20 in HBSS for 30 min. Cells were incubated with antibodies against the tight junction protein ZO-1 (1:50 dilution in block solution, Invitrogen, Carlsbad, CA) for 90 min, followed by a simultaneous incubation with goat-anti-rabbit-Alexa 568 conjugate (1:200, Life Technologies Europe BV, Bleiswijk, The Netherlands) and Phalloidin-Atto 488 (1:500), for actin filaments staining, for 30 min. Finally, DAPI nuclei staining (300 nM, Life Technologies Europe BV) was performed for 5 min. The modules were carefully cut open, and the extracted fibres were mounted on microscopy slides using Dako fluorescent mounting media (Dako Netherlands B. V., Heverlee, Belgium). The slides were examined under the Nikon confocal A1/super resolution N-STORM microscope (Nikon Instruments Europe B. V., Amsterdam, The Netherlands). Images were captured using the NIS-elements analysis software, version 4.40.000.

## 2.4 | Transepithelial barrier function

Paracellular permeability of the mature living membranes was quantified following the previously described method (Chevtchik et al., 2016). After washing the modules with Krebs–Henseleit buffer supplemented with HEPES (10 mM; KHH buffer), inulin-FITC (0.1 mg/ml in KHH buffer) was perfused at 18 ml/hr at 37 °C for 15 min. The inulin-FITC leakage was determined prior to perform functional IS transport. In some of the modules, the inulin-FITC leakage was determined before and after the IS transport experiment and after LPS or IFN- $\gamma$  exposure to assess the integrity of the monolayer after the functional tests.

## 2.5 | Functional organic anion transport

Transepithelial transport of IS through the HFM with matured ciPTEC was studied using a similar perfusion set-up as was used for the barrier function assay. First, fibres were preincubated in KHH buffer without or with probenecid (p) at concentrations 100  $\mu$ M (p100) or 500  $\mu$ M (p500) at 37 °C for 15 min. Next, the fibres were perfused using 100  $\mu$ M IS in KHH buffer in the presence or absence of inhibitors for 10 min at a flow rate of 18 ml/hr. Samples from both permeate and outlet were collected. IS concentrations were measured with a Jasco HPLC system equipped with a pump (PU-2080), an autosampler (PF-2020), UV/VIS detector (UV-2070), and fluorescence detector (FP-2020). The protocol was adapted from (Pavlenko et al., 2016). The excitation and emission wavelength for the fluorescence detector were set at 272 and 374 nm, respectively. The eluents used were ammonium formate (MW 63.06 g/mol) buffer 50 mM + 10% methanol at pH = 3.0. The flow rate was set at 0.5 ml/min.

## 2.6 | Production of the proinflammatory cytokines and human leukocyte antigens

The apical and basolateral sides of the living membrane were exposed to the following treatments depending on the experimental set-up: IFN- $\gamma$  300 ng/ml, LPS 10  $\mu$ g/ml. The production of IL-6, IL-8, TNF- $\alpha$ ,

and sHLA-Class I molecules in various stimulatory conditions was measured by means of enzyme-linked immuno-sorbent assays. Cell culture supernatants were collected from apical (external, volume ~3 ml) and basolateral (internal, volume ~0.4 ml) compartments after exposure to various stimulatory conditions, centrifuged for 10 min at 240 g, 4 °C, and stored at -80 °C. DuoSet® ELISA Development Systems kits (IL-6 #DY206, TNF- $\alpha$  #DY210, IL-8 #DY208; R&D systems, Abingdon, UK) and Human MHC Class-I kit (Proteintech, Chicago, IL, USA) were used to quantify the cytokine and sHLA-Class I levels, respectively, in cell culture supernatants according to manufacturer's instructions. The optical density was determined immediately using the iMark Microplate Absorbance Reader (Bio-Rad, Japan) set to 450 nm. Each sample was measured in duplicates, and quantification was done using Microplate Manager Software (version 6.0, Bio-Rad Laboratories, Hercules, CA, USA) capable of generating a four-parameter logistic (4-PL) curve-fit.

## 2.7 | Data analysis

Every experiment was performed at least in duplicate. The number of samples (*n*) measured is indicated in each figure legend. The results are presented as mean  $\pm$  standard deviation or standard error of the mean. Statistical analysis of the cell monolayer integrity and function was performed in the SPSS software (IBPM SPSS Statistics version 23.0) using a one-way analysis of variance (ANOVA) or Student's *t* test, where appropriate. Statistical analysis of the production of pro-inflammatory cytokines was performed in the GraphPad Prism software (GraphPad software, version 5.03; La Jolla, CA, USA), using either unpaired two-tailed test (for differences between two compartments in the same module) or one-way ANOVA followed by Tukey's multiple comparison test (for differences between treatments and different modules). A *p* value of <.05 was considered significantly different.

# 3 | RESULTS

## 3.1 | HFM characterization

The HFM were sterilized with steam to prevent risks of infection and coated with L-Dopa and collagen IV to allow ciPTEC adhesion and function. Prior to performing cell culturing experiments, the potential impact of sterilization and coating on the membrane transport properties was evaluated. Figure 1 compares the clean water flux (CWF) through the unsterilized or sterilized, and uncoated or coated HFM at different pressures. The steam sterilization did not affect the permeance of the uncoated membranes ((19.2  $\pm$  0.9)·10<sup>3</sup> L/(m<sup>2</sup>·h<sup>1</sup>·bar<sup>1</sup>)) unsterilized versus (18.9  $\pm$  0.8)·10<sup>3</sup> L/(m<sup>2</sup>·h<sup>1</sup>·bar<sup>1</sup>) sterilized. The permeance was slightly decreased when the double coating was applied on the sterilized HFM ((16.9  $\pm$  0.7)·10<sup>3</sup> L/(m<sup>2</sup>·h<sup>1</sup>·bar<sup>1</sup>)) compared with the unsterilized HFM ((19.0  $\pm$  0.3)·10<sup>3</sup> L/(m<sup>2</sup>·h<sup>1</sup>·bar<sup>1</sup>)) but remains high. This may be due to increased wettability of the membranes after sterilization, which favours the coating deposition and results in a slight pore occlusion. The SEM analysis shows no difference between the surfaces and cross sections of the uncoated and coated

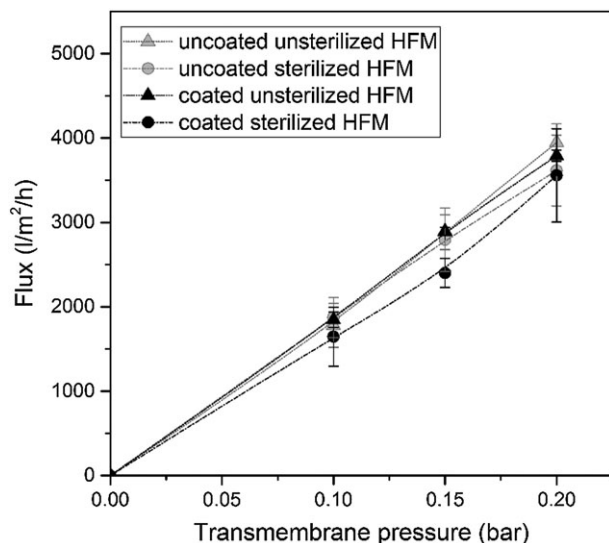


**FIGURE 1** Hollow fibre membrane (HFM) permeability. Clean water fluxes (CWFs) for unsterilized and sterilized HFM, with and without coating. The slope of the CWFs as a function of the pressure gives the HFM permeance. Data are shown as mean  $\pm$  standard deviation of three or four samples

HFM (see Figures S1 and S2). Overall, these results indicate that the high HFM permeance is preserved even after the sterilization and coating.

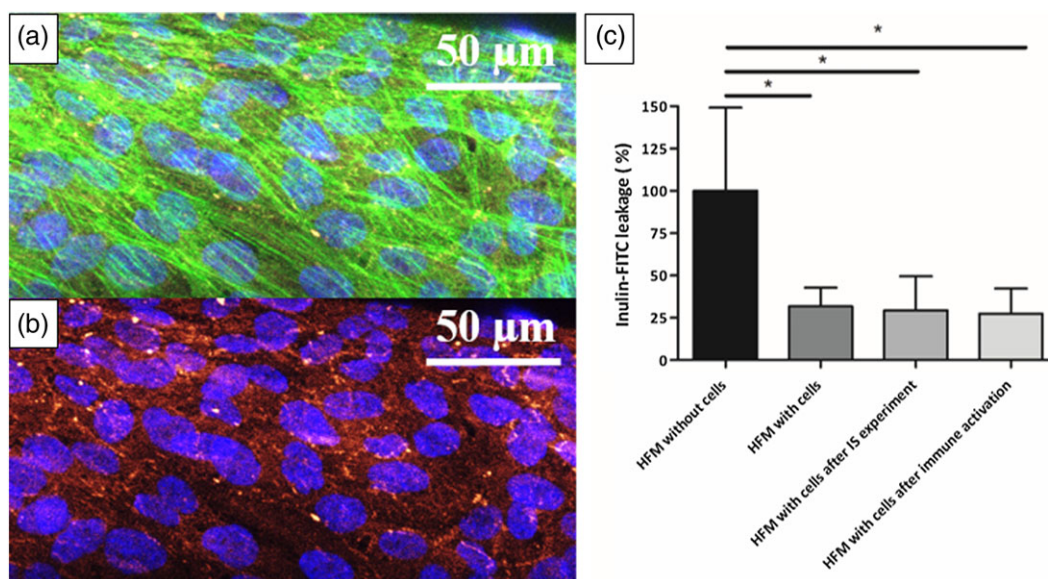
### 3.2 | Cell monolayer integrity and function

Figure 2a,b shows representative images of matured OAT-expressing ciPTEC cultured on MicroPES HFM. The applied L-Dopa (20 hr) and collagen IV (2 hr) coating supports the formation of a uniform ciPTEC monolayer. The abundant expression of the ZO-1 (Figure 2b) is

demonstrative for the presence of tight junctions between the cells. In addition to a polarized epithelial barrier, the tight junction proteins contribute to fluid and ion homeostasis mediated by paracellular transport (Kirk, Campbell, Bass, Mason, & Collins, 2010). Besides, cytoskeleton (actin) staining (Figure 2a) shows that the cells have proper shape, structure, and morphology, additionally confirming the epithelial character of the cell monolayer.

Inulin transport through the mature cell monolayer occurs in a nonactive manner, via diffusion through the intercellular junctions. Therefore, the inulin-FITC leakage test is representative of the monolayer tightness (Schophuizen et al., 2015). For a tight cell monolayer, inulin-FITC leakage is expected to be a lot lower than through HFM without cells. Figure 2c presents the inulin-FITC leakage through the tested HFM, for which the fibres without cells are set to 100%. The leakage of the HFM with a ciPTEC monolayer is as low as  $32 \pm 11\%$ . The data presented here arise from four experiments and 32 different modules.

We next assessed the activity of the transporter responsible for anionic urinary uraemic toxin excretion, viz., OAT1, by perfusing the living membranes with IS in the absence or presence of the OAT1 inhibitor, probenecid. Figure 3a shows the scheme of the experimental setup, and Figure 3b shows the transport results where the IS transport alone through the cell monolayer was set at 100%. The IS transport is inhibited by  $\sim 50\%$  by both concentrations of probenecid (IS transport becomes  $48 \pm 20\%$  and  $50 \pm 15\%$  of the original intensity, for p100 and p500, respectively), suggesting maintained cell function. The inhibition of IS transport was comparable for both concentrations of probenecid, suggesting that the saturation of the transporters was reached. After the inhibition tests, the cell monolayer was still intact as suggested by the low inulin-FITC leakage of around 30% (see Figure 2c). The absolute values of the IS clearance are presented in Figure S4.



**FIGURE 2** Monolayer quality of ciPTEC cultured on hollow fibre membrane (HFM). (a,b) Representative confocal microscopy images of ciPTEC cultured on HFM with the DAPI staining of nuclei (blue), the cytoskeleton (green), and the immunostaining for ZO-1 (red). (c) Inulin-FITC paracellular leakage, ratio HFM with cells/HFM without cells. The data presented here arose from four experiments and 32 different modules. Data are presented as mean  $\pm$  standard deviation. \*  $p < .001$  using a one-way analysis of variance [Colour figure can be viewed at wileyonlinelibrary.com]

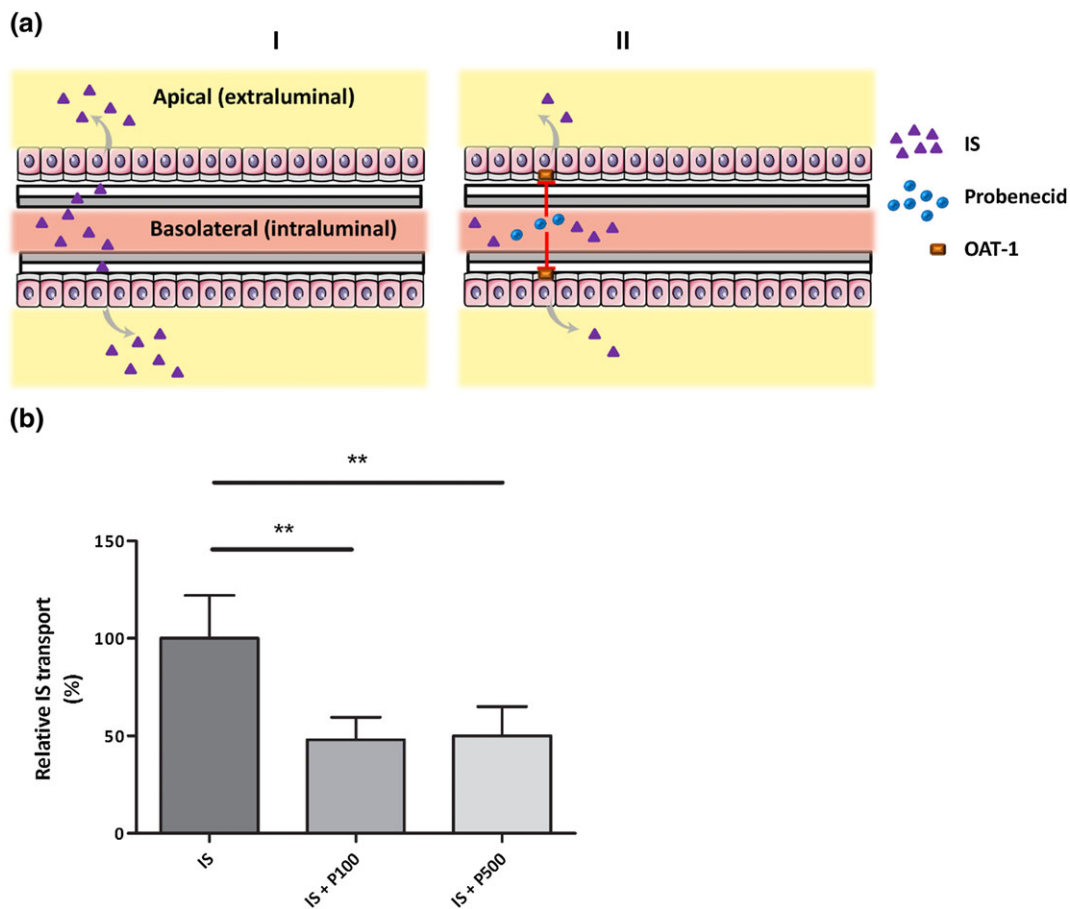


**FIGURE 3** Functional OAT1-mediated IS transport. (a) Schematic presentation of the experimental set-up of IS transepithelial transport in the absence (I) or presence (II) of probenecid. Adapted from (Jansen et al., 2016). (b) Quantification of IS transport (100  $\mu$ M) in the absence or presence of probenecid (concentration 100  $\mu$ M [p100] and 500  $\mu$ M [p500]) in matured cPTEC cultured on upscaled hollow fibre membrane. The perfusion lasted for 10 min. Data are normalized against IS transport in the absence of inhibitors and presented as mean  $\pm$  standard deviation of at least three modules per case, from two independent experiments. \* $p < .001$  using analysis of variance [Colour figure can be viewed at [wileyonlinelibrary.com](http://wileyonlinelibrary.com)]

### 3.3 | Production of the inflammatory and immune mediators

To assess whether the living membrane mediates an inflammatory or immune response, we evaluated the release of IL-6, IL-8, TNF- $\alpha$  and sHLA-Class I in both the extraluminal (apical) and in the intraluminal (basolateral) compartments. Figure 4a shows a schematic representation of the experimental set-up in the case of exposure to LPS; an identical set-up was used for the exposure to IFN- $\gamma$  and the release of sHLA-Class I. Figure 4b–e shows the release of proinflammatory cytokines IL-6, IL-8, and TNF- $\alpha$  and the sHLA-Class I.

Prior to exposure to LPS, the concentrations of IL-6 and IL-8 were found to be two to three times higher in the extraluminal compartment ( $(27 \pm 4) \cdot 10^3$  pg/ml and  $(10 \pm 1) \cdot 10^3$  pg/ml, respectively) than in the intraluminal compartment ( $(9 \pm 4) \cdot 10^3$  pg/ml and  $(4 \pm 1) \cdot 10^3$  pg/ml, respectively). When the cPTEC were directly exposed to LPS, the concentration of IL-6 and IL-8 increased in the extraluminal compartment (more than 10 times— $(496 \pm 267) \cdot 10^3$  pg/ml and  $(103 \pm 9) \cdot 10^3$  pg/ml, respectively). When LPS was administrated intraluminally, the extraluminal concentration of IL-6 and IL-8 increased slightly less (more than five times— $(100 \pm 15) \cdot 10^3$  pg/ml and  $(67 \pm 7) \cdot 10^3$  pg/ml,

respectively), most likely due to the small mass transfer resistance of the HFM. On the other hand, the intraluminal concentration of IL-6 remained the same for both extraluminal and intraluminal exposures to LPS ( $(19 \pm 4) \cdot 10^3$  pg/ml and  $(16 \pm 2) \cdot 10^3$  pg/ml, respectively). In similar conditions, the intraluminal concentration of IL-8 slightly increased: two times after extraluminal exposure and three times after intraluminal exposure ( $(9 \pm 2) \cdot 10^3$  pg/ml and  $(13 \pm 2) \cdot 10^3$  pg/ml, respectively).

The concentrations of TNF- $\alpha$  did not vary in all cases and remained very low (100–300 pg/mL), in agreement with our previous findings (Mihajlovic et al., 2017; Peters et al., 2015). If we, however, estimate the absolute amount of TNF- $\alpha$  in both compartments (based on the volume of each compartment, we observe that the amount of TNF- $\alpha$  is higher in the extraluminal than in the intraluminal compartment (Figure S3).

Similarly to TNF- $\alpha$ , the absolute levels of sHLA-Class I were rather low (concentrations  $< 20$  pg/ml) compared with normal serum levels (Rhynes et al., 1993; Zavazava, Leimenstoll, & Müller-Ruchholtz, 1990). Hence, in agreement with IL-6 and IL-8, the concentrations of sHLA-Class I were two to three times higher in the apical than in the basolateral compartment ( $15 \pm 6$  pg/ml and  $5 \pm 1$  pg/ml, respectively). The apical concentration of sHLA-Class I did not significantly change

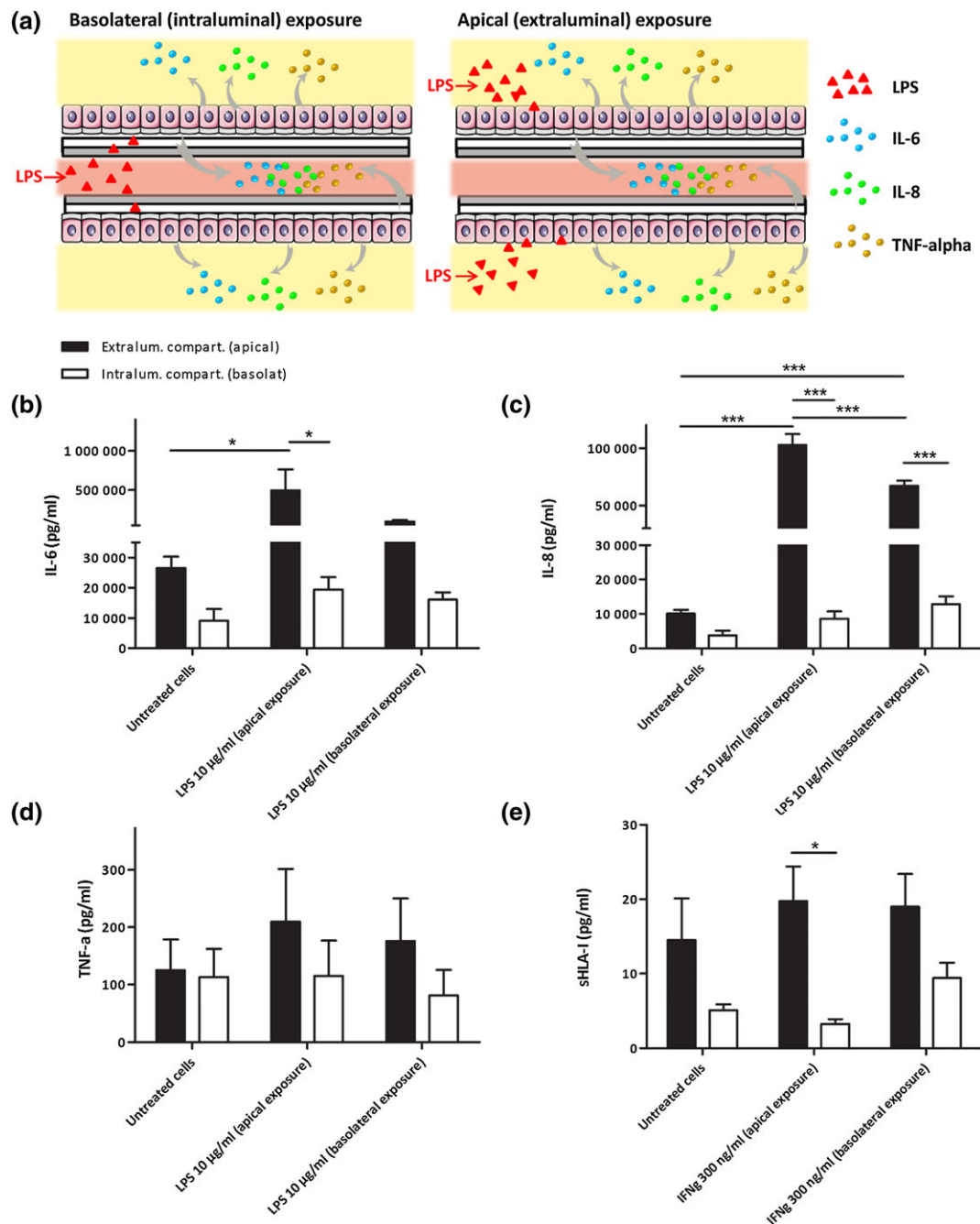


**FIGURE 4** Immune activation and production of proinflammatory cytokines and sHLA-Class I by matured ciPTEC on upscaled bioartificial kidney device. (a) Scheme of the experimental set-up used for studying the release of the proinflammatory cytokines, here after exposure to LPS and measure of IL-6, IL-8, and TNF- $\alpha$ ; an identical set-up was used in case of IFN- $\gamma$  treatment and sHLA-class I release. (b–e) Effect of 24-hr basolateral or apical exposure to LPS (10  $\mu$ g/ml; b–e) or IFN- $\gamma$  (300 ng/ml; e) on production of proinflammatory cytokines (IL-6, IL-8, and TNF- $\alpha$ ) and sHLA-Class I in the apical and basolateral compartments. Data are presented as mean  $\pm$  (standard error mean) of at least three modules per case, from two independent experiments. \* $p$  < .05 and \*\*\* $p$  < .001 using either unpaired two-tailed test (for differences between two compartments in the same module) or one-way anova followed by Tukey's multiple comparison test (for differences between treatments and different modules) [Colour figure can be viewed at [wileyonlinelibrary.com](http://wileyonlinelibrary.com)]

after the apical and basolateral exposures to IFN- $\gamma$  ( $20 \pm 5$  pg/ml and  $19 \pm 4$  pg/ml, respectively), although a slight (two-fold) increase was observed in the basolateral compartment after basolateral exposure ( $9 \pm 2$  pg/ml).

Overall, for all of the configurations tested, the concentration of IL-6, IL-8, and sHLA-Class I was higher in the extraluminal compartment, corresponding to dialysate, compared with the intraluminal one, which

would correspond to patient's blood. This conclusion holds true also for the absolute amounts of proinflammatory cytokines and sHLA-Class I in both compartments (see Figure S3). Finally, to assess the integrity of the cell monolayer during these tests, additional Inulin-FITC leakage tests were performed on the HFM after exposure to stimulatory conditions (LPS and IFN- $\gamma$ ), which was found to be rather low,  $27.4 \pm 14.9\%$  (Figure 3c), and similar to that before the stimulatory experiments.

## 4 | DISCUSSION

In this study, we developed upscaled (4 cm<sup>2</sup>) 3D modules containing double-coated MicroPES HFM supporting OAT1-expressing ciPTEC. With this system, we investigated the secretion of the proinflammatory cytokines IL-6 and IL-8 and sHLA-class by the cells in response to LPS or IFN- $\gamma$ , both basolaterally and apically, to mimic inflammatory conditions.

Confocal microscopic analysis of the ciPTEC monolayer after 7 days of maturation at 37 °C demonstrated regular nuclei, homogeneous cell structure and morphology, and abundant expression of the tight junction protein ZO-1. This underlines the epithelial character of the ciPTEC monolayer, which was confirmed further by limited inulin-FITC diffusion in agreement to earlier studies. Indeed, the earlier reported values—30  $\pm$  10% for an upscaled system (Chevtchik et al., 2016) and 31  $\pm$  9% (Jansen et al., 2015) for a small scale system—are identical to the Inulin-FITC leakage percentage—32  $\pm$  11%—reported here. In addition, the paracellular inulin-FITC leakage remained low after exposure to IS, LPS, or IFN- $\gamma$ , confirming the preservation of intact ciPTEC monolayers after the exposure to toxins and to inflammatory stimuli.

Our system demonstrated the active transport of IS, an anionic uraemic toxin from the family of the protein bound toxins (R. Vanholder, De Smet, Glorieux, Argiles, et al., 2003), reported as strongly linked to the fatal outcome in kidney patients (R. Vanholder, De Smet, Glorieux, & Dhondt, 2003; Vanholder et al., 2014). This active transport indicates the presence of functional OAT1-mediated transport. OAT1 is expressed at the basolateral membrane of PTEC, responsible for the uptake of anionic uraemic metabolites (Jansen et al., 2016; Nieskens et al., 2016) and is crucial for their renal elimination. Breast cancer resistance protein and MRP4 transporters, located on the apical membrane of PTEC, are responsible for the toxin excretion to the urine in the matured ciPTEC monolayer (Jansen et al., 2016). When the modules were incubated with probenecid, an inhibitor of OAT1, the transport of IS was reduced by approximately 40%. In comparison with the study performed on a short single HFM (Jansen et al., 2016), we also found a similar inhibition of the transport of IS (100  $\mu$ M) by probenecid 100  $\mu$ M: 48  $\pm$  31% (Jansen et al., 2016) in the single small HFM versus 55  $\pm$  6% now in the upscaled system,  $p < .001$ .

Finally, we studied the production of IL-6, IL-8, TNF- $\alpha$ , and sHLA-Class I, in basic conditions and in response to LPS and IFN- $\gamma$ , which we used to mimic inflammatory conditions as observed in uraemic syndrome. For the BAK, the production of proinflammatory cytokines is important for the activation of immune cells and propagation of inflammatory response usually present in Chronic kidney disease (CKD) patients, which could have undesirable effects. In most studies on BAK reported in the literature (Humes et al., 2002; Oo et al., 2011; Oo et al., 2013; Saito et al., 2012), the concentrations of cytokines were measured only from the waste (apical) compartment in vitro or the blood (basolateral) compartment in vivo. In our work, we measured the concentrations of proinflammatory cytokines in both apical and basolateral compartments, and we found that they were very low and their absolute values between extraluminal and basolateral compartment were significantly different.

Both in the absence and in the presence of LPS or IFN- $\gamma$ , the secretion of IL-6, IL-8, and of sHLA-Class I was significantly higher to the apical side—corresponding to dialysate compartment—compared with the basolateral secretion—corresponding to blood side.

Overall, our results indicate that the here described BAK device consists of functional polarized ciPTECs, which secrete higher amounts of cytokines and sHLA-Class-I molecules towards the dialysate compartment, thereby greatly reducing the risks associated with eventual proinflammatory and immunogenic effects of the cells.

## 5 | CONCLUSION AND OUTLOOK

This work presented the successful upscaling of the living membranes containing functional OAT1-mediated transport crucial for the removal of uraemic anionic toxins, such as IS. Importantly, the ciPTECs were fully polarized because the release of proinflammatory cytokines IL-6 and IL-8 and of sHLA-Class I was mainly oriented towards the apical side, or dialysate compartment, and not towards the basolateral side—corresponding to the side of the patient's body fluid.

The next step towards the development of a functional BAK device is to culture the cells while exposing them to a unidirectional flow with relative shear stress to mimic the natural kidney proximal tubule physiology. There is evidence that cell metabolism is stimulated when cells are cultured under dynamic conditions (Jang et al., 2013; Kim, Putnam, Kulik, & Mooney, 1998; Li & Cui, 2014; Sánchez-Romero, Meade, & Giménez, 2016; Weinbaum, Duan, Satlin, Wang, & Weinstein, 2010), which might further stimulate toxin removal. Moreover, a ciPTEC-based BAK device should ensure a sufficient toxin clearance for prolonged sessions. Here, the function of the living membrane was tested for 10 min. Future work should evaluate longer clearance periods, using plasma or blood samples from CKD patients. For the ciPTEC, the combination on L-Dopa and collagen IV worked best in the time scale of our experiments. If necessary, we would investigate in the future the application of renal ECM (e.g., from decellularised kidneys) to the fibres, too.

## ACKNOWLEDGEMENTS

This work was funded by the EU-FP7-PEOPLE-ITN-2012 Project BIOART (grant no 316690). The authors would like to gratefully thank the EuTox Working Group, of the European society, for artificial organs for its financial contribution. Natalia V. Chevtchik would like to gratefully thank the BioNanoLab of the University of Twente, The Netherlands, for its financial contribution. Igor Middel of Utrecht University is acknowledged for his help in IS measurements. The authors would like to gratefully thank Felix Broens and Convergence Industry B.V. for the technical assistance in the programme development for membrane properties characterization.

## CONFLICTS OF INTEREST

The authors have declared that there is no conflict of interest.

## ORCID

D. Stamatiadis  <http://orcid.org/0000-0002-2298-2442>

## REFERENCES

- Sánchez-Romero, N., Meade, P., & Giménez, I. (2016). Chapter 22—Microfluidic-based 3D models of renal function for clinically oriented research A2 - Laurence, Jeffrey. In *Translating regenerative medicine to the clinic* (pp. 315–334). Boston: Academic Press.
- Chevtchik, N. V., Fedecostante, M., Jansen, J., Mihajlovic, M., Wilmer, M., Rùth, M., ... Stamatialis, D. (2016). Upscaling of a living membrane for bioartificial kidney device. *European Journal of Pharmacology*, 790, 28–35. <https://doi.org/10.1016/j.ejphar.2016.07.009>
- Hsu, H. J., Yen, C. H., Wu, I. W., Hsu, K. H., Chen, C. K., Sun, C. Y., ... Lee, C. C. (2014). The association of uremic toxins and inflammation in hemodialysis patients. *PLoS One*, 9(7), e102691. <https://doi.org/10.1371/journal.pone.0102691>
- Humes, H. D., Fissell, W. H., Weitzel, W. F., Buffington, D. A., Westover, A. J., MacKay, S. M., & Gutierrez, J. M. (2002). Metabolic replacement of kidney function in uremic animals with a bioartificial kidney containing human cells. *American Journal of Kidney Disease*, 39(5), 1078–1087. <https://doi.org/10.1053/ajkd.2002.32792>
- Jang, K. J., Mehr, A. P., Hamilton, G. A., McPartlin, L. A., Chung, S., Suh, K. Y., & Ingber, D. E. (2013). Human kidney proximal tubule-on-a-chip for drug transport and nephrotoxicity assessment. *Integrative Biology (Camb)*, 5(9), 1119–1129. <https://doi.org/10.1039/c3ib40049b>
- Jansen, J., de Napoli, I. E., Fedecostante, M., Schophuizen, C. M., Chevtchik, N. V., Wilmer, M. J., ... Masereeuw, R. (2015). Human proximal tubule epithelial cells cultured on hollow fibers: living membranes that actively transport organic cations. *Scientific Reports*, 5, 16702. doi: <https://doi.org/10.1038/srep16702> (2015). doi: 10.1038/srep16702
- Jansen, J., Fedecostante, M., Wilmer, M. J., Peters, J. G., Kreuser, U. M., van den Broek, P. H., ... Masereeuw, R. (2016). Bioengineered kidney tubules efficiently excrete uremic toxins. *Scientific Reports*, 6, 26715. <https://doi.org/10.1038/srep26715>
- Jansen, J., Schophuizen, C. M., Wilmer, M. J., Lahham, S. H., Mutsaers, H. A., Wetzels, J. F., ... Masereeuw, R. (2014). A morphological and functional comparison of proximal tubule cell lines established from human urine and kidney tissue. *Experimental Cell Research*, 323(1), 87–99. <https://doi.org/10.1016/j.yexcr.2014.02.011>
- Kim, B. S., Putnam, A. J., Kulik, T. J., & Mooney, D. J. (1998). Optimizing seeding and culture methods to engineer smooth muscle tissue on biodegradable polymer matrices. *Biotechnology and Bioengineering*, 57(1), 46–54.
- Kirk, A., Campbell, S., Bass, P., Mason, J., & Collins, J. (2010). Differential expression of claudin tight junction proteins in the human cortical nephron. *Nephrology, Dialysis, Transplantation*, 25(7), 2107–2119. <https://doi.org/10.1093/ndt/gfq006>
- Krieter, D. H., Hackl, A., Rodriguez, A., Chenine, L., Moragues, H. L., Lemke, H. D., ... Canaud, B. (2009). Protein-bound uraemic toxin removal in haemodialysis and post-dilution haemodiafiltration. *Nephrology, Dialysis, Transplantation*, 25(1), 212–218. <https://doi.org/10.1093/ndt/gfp437>
- Li, Z., & Cui, Z. (2014). Three-dimensional perfused cell culture. *Biotechnology Advances*, 32(2), 243–254. <https://doi.org/10.1016/j.biotechadv.2013.10.006>
- Masereeuw, R., Mutsaers, H. A. M., Toyohara, T., Abe, T., Jhawar, S., Sweet, D. H., & Lowenstein, J. (2014). The kidney and uremic toxin removal: Glomerulus or tubule? *Seminars in Nephrology*, 34(2), 191–208. <https://doi.org/10.1016/j.semnephrol.2014.02.010>
- Meijers, B. K., Claes, K., Bammens, B., de Loor, H., Viaene, L., Verbeke, K., ... Evenepoel, P. (2010). p-Cresol and cardiovascular risk in mild-to-moderate kidney disease. *Clinical Journal of the American Society of Nephrology*, 5(7), 1182–1189. <https://doi.org/10.2215/CJN.07971109>
- Meyer, T. W., Walther, J., Pagtalunan, M. E., Martinez, A., Torkamani, A. L., Fong, P., ... Hostetter, T. (2005). The clearance of protein-bound solutes by hemofiltration and hemodiafiltration. *Kidney International*, 68(2), 867–877. <https://doi.org/10.1111/j.1523-1755.2005.00469.x>
- Mihajlovic, M., van den Heuvel, L. P., Hoenderop, J. G., Jansen, J., Wilmer, M. J., Westheim, A. J. F., ... Masereeuw, R. (2017). Allostimulatory capacity of conditionally immortalized proximal tubule cell lines for bioartificial kidney application. *Scientific Reports*, 7(1), 7103.
- Miyamoto, Y., Watanabe, H., Noguchi, T., Kotani, S., Nakajima, M., Kadowaki, D., ... Maruyama, T. (2011). Organic anion transporters play an important role in the uptake of p-cresyl sulfate, a uremic toxin, in the kidney. *Nephrology, Dialysis, Transplantation*, 26(8), 2498–2502. <https://doi.org/10.1093/ndt/gfq785>
- Nieskens, T. T., Peters, J. G., Schreurs, M. J., Smits, N., Woestenenk, R., Jansen, K., ... Masereeuw, R. (2016). A human renal proximal tubule cell line with stable organic anion transporter 1 and 3 expression predictive for antiviral-induced toxicity. *The AAPS Journal*, 18(2), 465–475. <https://doi.org/10.1208/s12248-016-9871-8>
- Oo, Z. Y., Deng, R., Hu, M., Ni, M., Kandasamy, K., Bin Ibrahim, M. S., ... Zink, D. (2011). The performance of primary human renal cells in hollow fiber bioreactors for bioartificial kidneys. *Biomaterials*, 32(34), 8806–8815. <https://doi.org/10.1016/j.biomaterials.2011.08.030>
- Oo, Z. Y., Kandasamy, K., Tasnim, F., & Zink, D. (2013). A novel design of bioartificial kidneys with improved cell performance and haemocompatibility. *Journal of Cellular and Molecular Medicine*, 17(4), 497–507. <https://doi.org/10.1111/jcmm.12029>
- Pavlenko, D., van Geffen, E., van Steenberghe, M. J., Glorieux, G., Vanholder, R., Gerritsen, K. G., & Stamatialis, D. (2016). New low-flux mixed matrix membranes that offer superior removal of protein-bound toxins from human plasma. *Scientific Reports*, 6, 34429. <https://doi.org/10.1038/srep34429>
- Peters, E., Geraci, S., Heemskerk, S., Wilmer, M. J., Bilos, A., Kraenzlin, B., ... Masereeuw, R. (2015). Alkaline phosphatase protects against renal inflammation through dephosphorylation of lipopolysaccharide and adenosine triphosphate. *British Journal of Pharmacology*, 172(20), 4932–4945. <https://doi.org/10.1111/bph.13261>
- Rhynes, K. V., McDonald, J. C., Gelder, F. B., Aultman, D. F., Hayes, J. M., McMillan, R. W., & Mancini, M. C. (1993). Soluble HLA Class I in the serum of transplant recipients. *Annals of Surgery*, 217(5), 485–491.
- Saito, A., Sawada, K., Fujimura, S., Suzuki, H., Hirukawa, T., Tatsumi, R., ... Kakuta, T. (2012). Evaluation of bioartificial renal tubule device prepared with lifespan-extended human renal proximal tubular epithelial cells. *Nephrology, Dialysis, Transplantation*, 27(8), 3091–3099. <https://doi.org/10.1093/ndt/gfr755>
- Sanechika, N., Sawada, K., Usui, Y., Hanai, K., Kakuta, T., Suzuki, H., ... Saito, A. (2011). Development of bioartificial renal tubule devices with lifespan-extended human renal proximal tubular epithelial cells. *Nephrology, Dialysis, Transplantation*, 26(9), 2761–2769. <https://doi.org/10.1093/ndt/gfr066>
- Schophuizen, C. M., de Napoli, I. E., Jansen, J., Teixeira, S., Wilmer, M. J., Hoenderop, J. G., ... Stamatialis, D. (2015). Development of a living membrane comprising a functional human renal proximal tubule cell monolayer on polyethersulfone polymeric membrane. *Acta Biomaterialia*, 14, 22–32. <https://doi.org/10.1016/j.actbio.2014.12.002>
- Sun, J., Wang, C., Zhu, B., Larsen, S., Wu, J., & Zhao, W. (2011). Construction of an erythropoietin-expressing bioartificial renal tubule assist device. *Renal Failure*, 33(1), 54–60. <https://doi.org/10.3109/0886022X.2010.536605>
- Takahashi, H., Sawada, K., Kakuta, T., Suga, T., Hanai, K., Kanai, G., ... Saito, A. (2013). Evaluation of bioartificial renal tubule device prepared with human renal proximal tubular epithelial cells cultured in serum-free medium. *Journal of Artificial Organs*, 16(3), 368–375. <https://doi.org/10.1007/s10047-013-0710-8>
- Tumlin, J., Wali, R., Williams, W., Murray, P., Tolwani, A. J., Vinnikova, A. K., ... Humes, H. D. (2008). Efficacy and safety of renal tubule cell therapy for acute renal failure. *Journal of the American Society of Nephrology*, 19(5), 1034–1040. doi: <https://doi.org/10.1681/ASN.2007080895>
- Vanholder, R., De Smet, R., Glorieux, G., & Dhondt, A. (2003). Survival of hemodialysis patients and uremic toxin removal. *Artificial Organs*, 27(3), 218–223.



- Vanholder, R., Schepers, E., Pletinck, A., Nagler, E. V., & Glorieux, G. (2014). The uremic toxicity of indoxyl sulfate and p-cresyl sulfate: A systematic review. *Journal of the American Society of Nephrology*, 25, 1–11. <https://doi.org/10.1681/ASN.2013101062>
- Vanholder, R., de Smet, R., Glorieux, G., Argiles, A., Baurmeister, U., Brunet, P., ... European Uremic Toxin Work, G. (2003). Review on uremic toxins: Classification, concentration, and interindividual variability. *Kidney International*, 63(5), 1934–1943. <https://doi.org/10.1046/j.1523-1755.2003.00924.x>
- Vanholder, R. C., Eloit, S., & Glorieux, G. L. (2015). Future avenues to decrease uremic toxin concentration. *American Journal of Kidney Diseases*, 67(4), 664–676. <https://doi.org/10.1053/j.ajkd.2015.08.029>
- Weinbaum, S., Duan, Y., Satlin, L. M., Wang, T., & Weinstein, A. M. (2010). Mechanotransduction in the renal tubule. *American Journal of Physiology*. Renal physiology, 299(6), F1220–F1236. <https://doi.org/10.1152/ajprenal.00453.2010>
- Wilmer, M. J., Saleem, M. A., Masereeuw, R., Ni, L., van der Velden, T. J., Russel, F. G., ... Levtchenko, E. N. (2010). Novel conditionally immortalized human proximal tubule cell line expressing functional influx and efflux transporters. *Cell and Tissue Research*, 339(2), 449–457. <https://doi.org/10.1007/s00441-009-0882-y>
- Zavazava, N., Leimenstoll, G., & Müller-Ruchholtz, W. (1990). Measurement of soluble mhc class i molecules in renal graft patients: A noninvasive allograft monitor. *Journal of Clinical Laboratory Analysis*, 4(6), 426–429. <https://doi.org/10.1002/jcla.1860040607>

## SUPPORTING INFORMATION

Additional supporting information may be found online in the Supporting Information section at the end of the article.

**Figure S1. SEM images of MicroPES HFM.** Magnification x900 and x950. (A, B, C) uncoated and (D, E, F) with L-Dopa and collagen IV

double coating. HFM (A, D) outside surface, (B-E) inside surface and (C, F) cross-section.

**Figure S2. SEM images of MicroPES HFM.** Magnification x9000. (A, B, C) uncoated and (D, E, F) with L-Dopa and collagen IV double coating. HFM (A, D) outside surface, (B-E) inside surface and (C, F) cross-section.

**Figure S3.** Immune activation and production of pro-inflammatory cytokines by matured ciPTEC on upscaled BAK. (A) Scheme of the experimental set up used for the study of the release of the pro-inflammatory cytokines, here after exposure to LPS and measure of IL-6, IL-8 and TNF- $\alpha$ ; an identical setup was used in case of IFN- $\gamma$  treatment and sHLA-class I release. (B, C, D, E) Effect of 24 h basolateral or apical exposure to LPS (10  $\mu$ g/ml) (B, C, D) or IFN- $\gamma$  (300 ng/ml) (E) on production of pro-inflammatory cytokines (IL-6, IL-8 and TNF- $\alpha$ ) and sHLA-class I in the apical and basolateral compartments. Data are presented as mean  $\pm$  (standard error mean; SEM) of at least 3 modules per case, from two independent experiments. \* $P < 0.05$ , \*\* $P < 0.01$  and \*\*\* $P < 0.001$  using either unpaired two-tailed test (for differences between two compartments in the same module) or one way ANOVA followed by Tukey's multiple comparison test (for differences between treatments and different modules).

**How to cite this article:** Chevtchik NV, Mihajlovic M, Fedecostante M, et al. A bioartificial kidney device with polarized secretion of immune modulators. *J Tissue Eng Regen Med*. 2018;12:1670–1678. <https://doi.org/10.1002/term.2694>